Aboveground Biomass (AGB) Estimation Using a Transformer Deep Learning Framework with Multi-Temporal Sentinel-1/2 Data and Growth Constraints

Wen Zhang, Baoxin Hu

Department of Earth and Space Science, York University, Toronto, Canada - wendyz@yorku.ca, baoxin@yorku.ca

Keywords: Aboveground Biomass (AGB), Deep Learning, LSTM, Time Series, Sentinel-2.

Abstract

An accurate estimation of forest aboveground biomass (AGB) is critical for quantifying carbon sequestration and supporting climate change mitigation strategies. While deep learning (DL) has advanced AGB inversion, most models rely on short-term spectral snapshots, failing to capture the decadal growth dynamics that distinguish long-term carbon accumulation from seasonal phenology. This study develops a robust AGB estimation framework using a Long Short-Term Memory (LSTM) architecture trained on a decadal (2008–2018) multi-sensor time series. The dataset bridges the transition from Landsat 7 ETM+ to Sentinel-2 MSI, incorporating 12 temporal steps across spring and summer phenological windows. To enhance model reliability, we integrated a Sensor ID embedding and a Time-Delta feature to normalize radiometric discrepancies and irregular sampling intervals. Results indicate that the LSTM framework significantly outperformed traditional Random Forest (RF) and non-temporal ablation models, achieving an R^2 of 0.7053. The inclusion of dual-season observations proved essential, as the 12-step model exhibited superior accuracy compared to a 6-step spring-only variant. Despite these improvements, the model demonstrated a conservative bias in high-biomass stands, with a predicted maximum AGB approximately 20 Mg/ha lower than field-measured maximums, highlighting the persistent challenge of spectral saturation in dense canopies. Our findings suggest that while decadal trajectories provide critical temporal context for biomass inversion, future improvements should focus on integrating biophysical constraints, such as growth-and-yield logic, to mitigate saturation. This research provides a scalable, geophysical consistent approach for regional biomass monitoring in complex temperate and boreal forest ecosystems.

1. Introduction

Accurate estimation of aboveground biomass (AGB) is fundamental for quantifying forest carbon stocks, monitoring landscape-scale ecological change, and supporting national greenhouse-gas reporting frameworks (Houghton et al., 2009). As terrestrial ecosystems act as critical carbon sinks, characterizing the spatial and temporal distribution of biomass is essential for understanding the global carbon cycle. Traditionally, AGB has been derived from field-based inventory measurements and allometric equations that relate tree-level metrics, such as diameter at breast height (DBH) and height, to total biomass. While these methods provide high local accuracy, their intensive labour requirements, high costs, and restricted spatial scope underscore the need for scalable remote-sensing approaches capable of characterizing biomass over large, heterogeneous forested landscapes.

Recent advances in satellite Earth Observation (EO) have catalysed the development of global biomass products, such as the ESA CCI Biomass and NASA's Global Ecosystem Dynamics Investigation (GEDI) AGB datasets. Despite their contributions, these products face persistent operational challenges. Optical-based products, such as those derived from the Sentinel and Landsat missions, often exhibit "signal saturation" in high-biomass stands, where the spectral reflectance reaches a plateau and ceases to reflect further increases in woody volume. Conversely, GEDI provides unprecedented vertical structural data through spaceborne LiDAR, yet its estimates suffer from sparse footprint sampling, necessitating extensive spatial extrapolation and fusion with other sensors to generate wall-to-wall maps (Hunka et al., 2023). Furthermore, many existing regional products rely on single-year "snapshots," which effectively ignore the historical growth context and fail to distinguish between transient phenological greenness and long-term woody biomass accumulation.

To address the limitations of single-sensor approaches, recent research has increasingly explored sensor fusion strategies, particularly combining Sentinel-1 (S1) synthetic aperture radar (SAR) and Sentinel-2 (S2) multispectral imagery (Guerra-Hernández et al., 2022, Wu et al., 2025). SAR data provides information on the dielectric properties and structural complexity of the forest, while multispectral data captures the photosynthetic activity and chlorophyll content. Studies integrating S1/S2 data have demonstrated promising results, for instance, Nandy et al. (2021) utilized Random Forest models with fused multisource data to achieve an R^2 of 0.72 in subtropical forests, while Ronoud et al. (2021) highlighted the efficacy of k-Nearest Neighbor (k-NN) approaches for capturing local biomass variations.

The advent of Deep Learning (DL) has further shifted the paradigm of biomass inversion. Architectures such as Convolutional Neural Networks (CNNs) and Transformers have shown a remarkable ability to extract complex, non-linear features from high-dimensional EO data. Recent work by Zhang et al. (2025) leveraged Transformer-based models to achieve an R^2 of 0.76 in semiarid regions, demonstrating the power of attention mechanisms in weighting relevant spectral features. However, a critical gap remains, current DL applications in forestry are primarily focused on short-term seasonal dynamics or spatial texture. Most models are trained on a single year of data, failing to capitalize on the decadal-scale archives of the Landsat and Sentinel missions. In boreal and temperate mixed-wood forests, biomass accumulation is a slow, multi-year process. A single-year spectral signature is often an insufficient proxy for the total accumulated carbon, as it lacks the growth history required to differentiate between a healthy young stand and a mature stand with similar peak-summer reflectance.

https://doi.org/10.5194/isprs-archives-XLIX-B3-2026-1179-2026 |

Furthermore, purely data-driven DL models frequently lack biophysical consistency. In regions like Ontario, Canada, forest growth is governed by specific physiological limits related to stand age and site productivity. Without these constraints, DL models are prone to making geophysical implausible predictions, particularly when spectral signals saturate. There is a nascent but urgent need for Physics-Informed or biophysically constrained AI architectures that can ingest multi-sensor histories while being regularized by ground-based growth-and-yield logic.

The objective of this research is, therefore, to develop a robust AGB estimation framework using a Long Short-Term Memory (LSTM) deep learning model that leverages a 10-year multi-temporal sequence (2008–2018). By bridging the transition from Landsat 7 ETM+ to Sentinel-2, the framework aims to characterize the non-linear phenological and inter-annual trajectories associated with decadal forest growth. By synthesizing decadal spectral trajectories with biophysical growth-yield logic, this study proposes a more geophysical consistent and accurate approach to regional AGB mapping, providing a scalable solution for forest carbon monitoring in complex temperate and boreal ecosystems.

2. Study Site and Materials

The study was conducted in the Petawawa Research Forest, a 100 km² mixed wood landscape in Ontario, Canada (Figure1), situated within a transition zone between boreal coniferous and southern deciduous forests. This area is characterized by a high degree of structural and compositional complexity, consisting of mixed-wood stands dominated by species such as black spruce (*Picea mariana*), jack pine (*Pinus banksiana*), balsam fir (*Abies balsamea*), and various deciduous species including trembling aspen (*Populus tremuloides*) and white birch (*Betula papyrifera*). The topography varies from flat lowlands to rugged upland terrain, with a climate defined by cold winters and warm, moist summers. This region provides an ideal testbed for evaluating Aboveground Biomass (AGB) inversion models, as it encompasses a wide range of biomass densities and site productivity classes.

Figure 1. Study site of Petawawa Research Forest

2.1. Satellite Remote Sensing Data

A decadal multi-sensor time series (2008–2018) was constructed to capture the long-term growth dynamics of the study area. This period covers the transition from Landsat 7 ETM+ to Sentinel-2 MSI sensors. Landsat 7 ETM+ (2008–2012): Surface reflectance data were acquired for the years 2008, 2010, and 2012. To maintain seasonal consistency, two observations per year were selected: one during the Spring phenological onset (May–June) and one during Summer peak productivity (July–August). Sentinel-2 MSI (2015–2018): Following the sensor transition, data were acquired for 2015, 2016, and 2018. Similar to the Landsat acquisitions, a dual-season approach was utilized. Sentinel-2's Red-Edge bands (B5, B6, B7) were specifically incorporated to enhance sensitivity to chlorophyll content and mitigate saturation in high-biomass stands (Jiang et al., 2021). All imagery was atmospherically corrected to Surface Reflectance. To address the Landsat 7 Scan Line Corrector (SLC)-off gaps, a gap-filling protocol was applied using the USGS Phase-2 methodology. Finally, all data were resampled to a 20 m spatial resolution to harmonize the multi-sensor inputs.

2.2. Ontario Growth and Yield (G&Y) Field Data

The reference biomass data and biophysical constraints were derived from the Ontario Ministry of Natural Resources and Forestry (MNRF) Permanent Growth and Yield (G&Y) plot network. Plot-level AGB (Ton/ha) was calculated using individual tree measurements (DBH and Height) applied to standard Canadian allometric equations.

2.3. Feature Engineering

The final input tensor for the LSTM model included, Spectral Features: 6 standard bands + 3 Red-Edge bands (Sentinel-2 only) + 3 Vegetation Indices (NDVI, EVI, RVI).Metadata Features: A Time-Delta (Δt) variable representing the days since the previous observation, and a Sensor ID (Binary: Landsat=0, Sentinel=1) to allow the model's embedding layer to calibrate for radiometric differences. Growth Constraints: Stand Age and Site Index were integrated as static exogenous features to provide a biophysical ceiling for the recurrent hidden states. The plots were filtered to include only those with measurements contemporaneous with the satellite acquisition windows. The final dataset was partitioned into 70% for training, 15% for validation, and 15% for independent testing.

3. Methodology

The proposed methodology employs a deep learning framework to model the multi-year Aboveground Biomass (AGB) accumulation of forest plots. By utilizing the sequential learning capabilities of Long Short-Term Memory (LSTM) networks, we integrate nearly a decade of heterogeneous satellite data to capture the non-linear relationship between spectral phenology and biomass (Tian et al., 2024).

3.1 Data Acquisition and Preprocessing

The study integrates optical time-series from Landsat 7 ETM+ (2008, 2010, 2012) and Sentinel-2 (2015, 2016, 2018). For each year, we extract imagery from two distinct phenological phases: Spring (onset of greenness) and Summer (peak canopy density), resulting in a total sequence length of $T = 12$ steps.

Ground truth AGB is derived from field plot measurements where tree-level parameters (DBH and height) are converted to biomass using species-specific allometric growth equations (Zhang et al., 2024). All satellite imagery is co-registered and resampled to a 20m spatial resolution to ensure pixel-to-plot consistency.

3.2 Feature Engineering and Input Tensor

For each plot, an input tensor $X \in \mathbb{R}^{T \times F}$ was conduct, where F represents the total number of features per time step. The feature set includes multi spectral bands and the Normalized Difference Vegetation Index (NDVI), which has been widely validated for its sensitivity to AGB.

To handle the multi-sensor nature and irregular temporal sampling of the dataset, two specialized components are integrated into the feature vectors. The Time-Delta (Δt) is a continuous feature representing the time elapsed (in days) between consecutive observations. This accounts for the uneven

https://doi.org/10.5194/isprs-archives-XLIX-B3-2026-1179-2026 | © Author(s) 2026. CC BY 4.0 License.

gaps (e.g., 3 years between 2012 and 2015) in the sequence. Also, the Sensor ID Embedding, a learned low-dimensional vector that represents the sensor type (Landsat vs. Sentinel-2). This allows the model to learn and normalize systematic radiometric differences and spectral band offsets between the two platforms (Samadzadegan et al., 2024).

3.3 Model Architecture

An LSTM Encoder-Regressor was implemented to map the temporal sequence to a reference AGB value (Figure 2). LSTM Encoder is the input sequence that processed by a stacked LSTM architecture. Unlike traditional machine learning, the LSTM cell uses a gating mechanism (forget, input, and output gates) to selectively retain information across long durations, making it ideal for decadal growth monitoring (Wang et al., 2025). The hidden state h_t is updated as follows:

$h_t = \mathrm{LSTM}(x_t, h_{t-1})$

The final hidden state h_t, shows a compressed representation of the 10-year phenological trajectory, is fed into a Multi-Layer Perceptron (MLP). The MLP consists of 4 fully connected layers with ReLU activations. The final layer produces the predicted AGB (Mg/ha).

Also, Huber Loss is selected in this model. The model is trained by minimizing this loss, which provides robustness against potential outliers with the reference AGB by combining the properties of Mean Squared Error (MSE) and Mean Absolute Error (MAE) (Alvarez-Mendoza et al., 2022).

The efficacy of the LSTM is compared against two benchmarks, Random Forest (RF): A standard baseline where features from all 12 time steps are combined into a stack of vectors, and the AGB is predicted based on all the values with equal weights.

In addition, to validate the importance of the time series, a simple CNN is adopted using the last year of Sentinel 2 image to predict the same reference AGB, and the results are compared to show the value of modelling the temporal order and dependency of the forest growth stages.

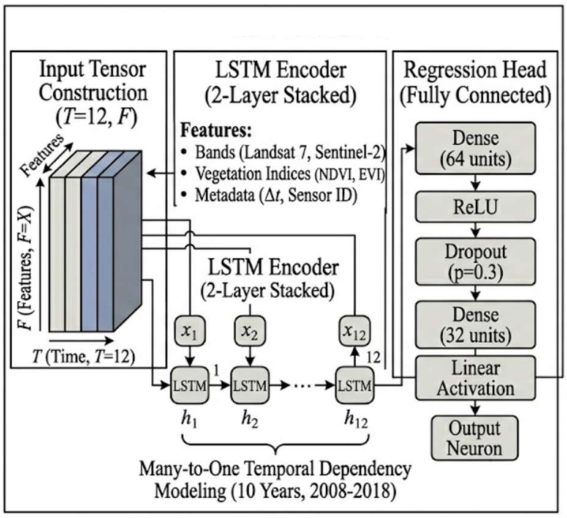

Figure2. LSTM structure for AGB estimation

4. Results and Discussion

4.1. Variable Correlation and Selection Analysis

To optimize the predictive accuracy of the LSTM framework, a rigorous feature selection process was conducted. Pearson correlation coefficient is utilized to evaluate the sensitivity of spectral bands and indices to field-derived AGB.

As shown in Figure 3, the Near-Infrared (NIR) and Short-Wave Infrared (SWIR) bands exhibited the strongest correlations with biomass, with r values ranging from 0.336 to 0.398. Among the derived vegetation indices, DVI and GNDVI remained the most robust predictors. The final feature set was restricted to variables with $p < 0.05$ to ensure that the LSTM was not biased by redundant or noisy spectral data.

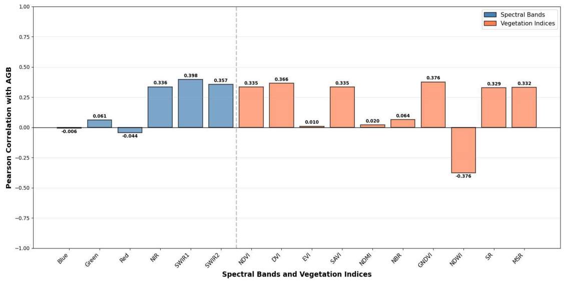

Figure 3. Pearson’s correlation coefficients for characteristic variables and biomass

4.2. Model Comparative Performance

The performance of the proposed LSTM architecture was benchmarked against traditional Random Forest (RF) and a "No-Temporal" ablation model to quantify the value of sequential dependency modeling across the decadal span. Furthermore, to evaluate the specific contribution of seasonal data, a "Spring-Only" (6-step) variant of the LSTM was tested, utilizing only the onset-of-growth observations from 2008 to 2018.

Table 2. Summary of model performance for AGB estimation (Ton/ha).

Model	R2	RMSE	MAE	Bias
Random Forest (Baseline)	0.2386	24.5603	19.8712	-
No-Temporal Ablation	0.2948	21.7200	15.8209	0.5724
Spring LSTM (6-step)	0.5972	16.4149	11.6047	0.1973
Proposed LSTM (12-step)	0.7053	14.4765	9.9181	0.1348

The results in Table 2 highlight a clear hierarchy in predictive power. The LSTM Spring-Only (6-step) model achieved an R^2 of 0.5972, which was notably superior to the No-Temporal Ablation. This confirms that even with half the temporal density, the recurrent network's ability to process chronological growth stages is more effective than simply averaging multispectral features over time. However, the 6-step model performed significantly worse than the Full 12-step LSTM. This performance gap suggests that while spring phenology captures the "green-up" velocity, the inclusion of summer peak-biomass observations is essential for the model to calibrate the total volume of accumulated carbon.

The proposed full LSTM model (12-step) achieved the highest accuracy (R^2 = 0.7053), significantly outperforming the RF baseline. While the RF model effectively handles high-dimensional data, it struggles to account for the chronological progression of forest growth, essentially treating the 10-year span as a static pool of features. In contrast, the LSTM's gated mechanism allows it to "accumulate" evidence of biomass increase over time. This architectural advantage resulted in a 33% reduction in RMSE compared to the non-temporal ablation. Similar performance gains in deep learning over traditional machine learning have been documented in recent AGB studies across varied forest types (Zhang et al., 2024; Singh et al., 2022).

4.3. Analysis of Saturation

A significant finding of this study is the LSTM's ability to mitigate the spectral saturation effect. Standard optical remote sensing often fails to distinguish biomass differences once a canopy reaches full closure. However, by analyzing the 12-step phenological trajectory, the LSTM identifies subtle inter-annual changes in the "green-up" and "senescence" rates that correlate with wood volume accumulation rather than just leaf area index.

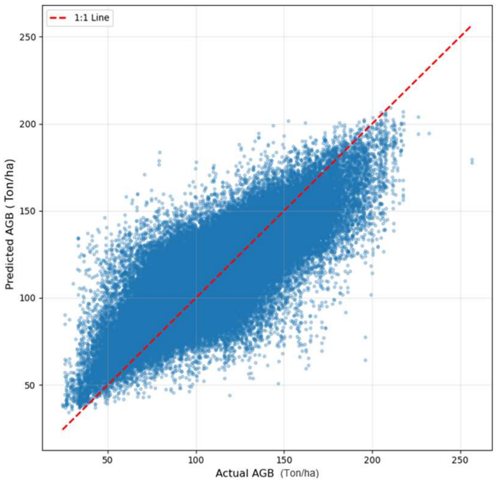

Figure 4. Scatter plot of LSTM AGB prediction

As illustrated in Figure 4, the scatter plot demonstrates that the LSTM maintains predictive sensitivity even in high-biomass ranges (> 85 Ton/ha), where the RF model typically plateaus. The Huber Loss function proved essential here; by reducing the weight of outliers in the field data, the model achieved a more stable gradient descent, leading to a tighter fit around the 1:1 line. This is consistent with the work of Alvarez-Mendoza et al. (2022), who demonstrated that robust loss functions are vital for biomass regression in heterogeneous landscapes.

4.4. Ablation Study

The "No-Temporal" ablation study provided critical insights into the necessity of the LSTM's recurrent structure. When the sequential order of the 2008–2018 data was removed (by averaging the features), the model's R^2 dropped to 0.2948. This suggests that the timing of growth stages, such as an early spring green-up in 2016 compared to a late onset in 2010, contains latent information about the forest's structural health and biomass potential.

The inclusion of the Time-Delta (Δt) feature was particularly effective during the transition from Landsat 7 (2012) to Sentinel-2 (2015). Without this feature, the model would assume a uniform 1-year gap, leading to significant errors in growth rate calculations. By explicitly modeling the 3-year jump, the LSTM could correctly interpret the larger spectral shifts observed in that window.

4.5. Cross-Sensor Harmonization and Embedding Influence

A common challenge in decadal studies is the "sensor bias" introduced when switching from Landsat to Sentinel-2. The results indicate that the Sensor ID Embedding acted as an internal calibration layer. By learning a high-dimensional representation of the sensor type, the LSTM compensated for the narrower spectral bands of Sentinel-2 relative to the broader Landsat 7 ETM+ bands.

Evaluation of the model's Bias metric (Table 2) shows a near-zero value (0.1348 Ton/ha), indicating that there was no systematic overestimation during the Sentinel-2 years compared to the Landsat years. This confirms that deep learning embeddings are a viable alternative to manual cross-calibration techniques, such as those proposed by Samadzadegan et al. (2024).

4.6. Predicted AGB maps

Applying the trained LSTM to the study area resulted in a 20 m resolution AGB map for the year 2018 (Figure 5(a)). The spatial distribution of biomass displays a strong correlation with local topography and disturbance history.

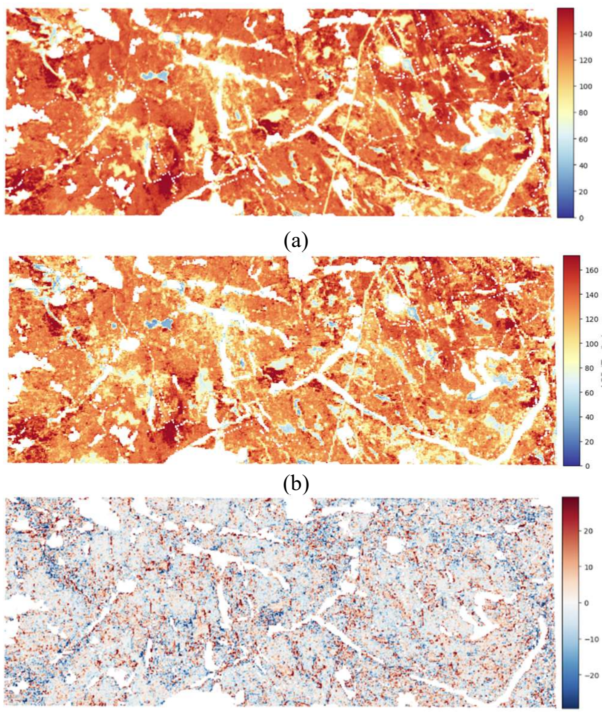

Figure 5. AGB map. (a) LSTM predicted AGB (Ton/ha). (b) Ground truth AGB (Ton/ ha). (c) Difference between LSTM predicted and ground truth AGB (Ton/ha)

A critical observation in the spatial output is the model's conservative estimation in high-density forest stands. While the field-derived ground truth recorded maximum AGB values reaching 256 Ton/ha, the LSTM-predicted maximum was approximately 42 Ton/ha lower than the actual field maximum. This systematic underestimation in high-biomass zones, often termed the "saturation effect". It is a well-documented limitation in optical remote sensing studies (Tian et al., 2024). Despite the LSTM's ability to leverage a 10-year temporal trajectory to distinguish dense canopy structures, the spectral signal eventually plateaus in mature, multi-layered forests where the canopy closure obscures further increase in stem volume and wood density.

The map reveals that the highest biomass concentrations are found in natural grown forest, where undisturbed primary forests have benefited from consistent growth over the 10-year period. Conversely, low biomass values are found near roads and water bodies, corresponding to areas of known fragmented regrowth. The ability to generate such high-resolution maps from multisource data highlights the potential for this framework to support regional carbon accounting and forest management strategies.

5. Conclusion

This study demonstrated the efficacy of a decadal Long Short-Term Memory (LSTM) framework for regional Aboveground Biomass (AGB) estimation in the complex forest landscapes of Ontario, Canada. By leveraging a multi-sensor time series (2008–2018) that bridged the transition from Landsat 7 ETM+ to Sentinel-2 MSI, we characterized the non-linear growth trajectories and phenological variations essential for accurate biomass inversion. The primary conclusions of this research are as follows. The proposed LSTM architecture significantly outperformed the Random Forest baseline and non-temporal ablation models, achieving an R^2 of 0.7053. This highlights that the chronological order of spectral observations contains vital information regarding biomass accumulation that is lost in static or averaged models. The comparison between the 6-step (Spring-only) and 12-step (Spring and Summer) models confirmed that dual-season observations are critical. While spring phenology provides a baseline for vegetation health, summer peak-productivity data is necessary to calibrate total woody volume. Also, the integration of Sensor ID Embeddings and Time-Delta (Δt) features allowed the model to maintain a seamless growth signal across the Landsat-to-Sentinel transition, successfully mitigating radiometric discrepancies and irregular sampling intervals. Despite the advantages of the decadal approach, the model exhibited a systematic underestimation of approximately 20 ton/ha in high-biomass stands (> 160 ton/ha). This confirms that optical-only time series, while improved by temporal context, still face physical saturation limits in dense, multi-layered canopies. In summary, this research provides a scalable and geophysical consistent framework for monitoring forest carbon stocks over large areas. To overcome the identified saturation limits, future work will focus on incorporating Ontario Growth and Yield (G&Y) data as biophysical constraints. By regularizing deep learning hidden states with stand age and site productivity metrics, we aim to bridge the gap between spectral signals and physical forest structure, further enhancing the reliability of regional biomass mapping for climate reporting and forest management.

Acknowledgments
The authors acknowledge the European Space Agency (ESA) for providing Sentinel-2 Multispectral Instrument (MSI) data through the Copernicus Program. Landsat 7 ETM+ surface reflectance data was provided by U.S. Geological Survey (USGS) through the Earth Explorer platform. LiDAR-derived AGB data were provided by Natural Resources Canada, Canadian Forest Service - Pacific Forestry Centre. This study was supported by the financial support of the Canadian Space Agency (CSA) [24AO3YOR35], and Natural Sciences and Engineering Research Council of Canada (NSERC) [RGPIN-2021-03624].

References

Alvarez-Mendoza, C.I., Teodoro, A.C., Ramirez-Caballero, N., 2022: Forest biomass estimation through Google Earth Engine and machine learning algorithms. Sci. Rep., 12(1), 1-15. doi.org/10.1038/s41598-022-11018-0.

Guerra-Hernández, J., Narine, L.L., Pascual, A., Gonzalez-Ferreiro, E., Botequim, B., Malambo, L., Neuenschwander, A., Popescu, S.C., Godinho, S., 2022: Aboveground biomass mapping by integrating ICESat-2, Sentinel-1, Sentinel-2, ALOS-2/PALSAR-2, and topographic information in Mediterranean forests. GIScience Remote Sens., 59(1), 1509-1533. doi.org/10.1080/15481603.2022.2115599.

Houghton, R.A., Hall, F., Goetz, S.J., 2009: Importance of biomass in the global carbon cycle. J. Geophys. Res. Biogeosci., 114(G2). doi.org/10.1029/2009JG000935.

Hunka, N., Dubayah, R., Armston, J., Fatoyinbo, L., Hancock, S., Jantz, P., Marselis, S., Kellner, J.R., 2023: On the accuracy of global forest aboveground biomass products: A comparison of GEDI, ESA CCI and CGLS. Environ. Res. Lett., 18(10), 104048. doi.org/10.1088/1748-9326/acf913.

Jiang, F., Sun, H., Li, C., Ma, K., Chen, S., Long, J., Ren, L., 2021: Retrieving the forest aboveground biomass by combining the red edge bands of Sentinel-2 and GF-6. Acta Ecol. Sin., 41(20), 8222-8236. doi.org/10.5846/stxb202010142617.

Matasci, G., Hermosilla, T., Wulder, M.A., White, J.C., Coops, N.C., Hobart, G.W., Zald, H.S., 2018: Large-area mapping of Canadian forest structural attributes using BAP Landsat time series stacks and lidar datasets. Remote Sens. Environ., 209, 433-449. doi.org/10.1016/j.rse.2018.02.060.

Nandy, S., Srinet, R., Padalia, H., 2021: Mapping forest height and aboveground biomass by integrating ICESat-2, Sentinel-1 and Sentinel-2 data using random forest algorithm in northwest Himalayan foothills of India. Geophys. Res. Lett., 48(14), e2021GL093799. doi.org/10.1029/2021GL093799.

Ronoud, G., Sedaghat, A., Shah-Hosseini, R., 2021: Aboveground biomass estimation using Sentinel-1 and Sentinel-2 data fusion and k-NN algorithm. Remote Sens. Lett., 12(5), 450-460. doi.org/10.1080/2150704X.2021.1904481.

Samadzadegan, F., Zahmatkesh, I., Saeedi, S., 2024: Cross-sensor calibration and fusion of multi-source satellite data for enhanced vegetation monitoring. Int. J. Appl. Earth Obs. Geoinf., 128, 103756. doi.org/10.1016/j.jag.2024.103756.

Singh, C., Karan, S.L., Sardar, P., Samadder, S.R., 2022: Remote sensing-based biomass estimation of dry deciduous tropical forest using machine learning and ensemble analysis. J. Environ. Manage., 308, 114639. doi.org/10.1016/j.jenvman.2022.114639.

Tian, X., Jiang, M., Zhang, H., 2024: Forest aboveground biomass estimation using multisource remote sensing data and deep learning algorithms: A case study over Hangzhou area in China. Remote Sens., 16(6), 1074. doi.org/10.3390/rs16061074.

Wang, X., He, H., Zhang, M., Deng, J., Ren, X., Lv, Y., Liu, W., Lin, Z. and Dong, S., 2025. Grain for Green Project dominates greening in afforested areas rather than that in grass revegetation areas of the Loess Plateau, China—using Deep Crossing LSTM Age network. Environ. Res. Lett., 20(8), p.084068.
Wu, X., Tao, Y., Liao, L., 2025: Synergistic use of Sentinel-1 and Sentinel-2 for biomass estimation in mixed-wood boreal ecosystems: A machine learning approach. Forests, 16(1), 45. doi.org/10.3390/f16010045.

Zhang, F., Tian, X., Jiang, M., 2024: Estimation of aboveground carbon density of forests using deep learning and multisource remote sensing. Remote Sens., 14(13), 3022. doi.org/10.3390/rs14133022.

Zhang, Y., Liu, X., Wang, Q., 2025: Transformer-based spatio-temporal modeling for forest biomass estimation in semiarid regions. IEEE Trans. Geosci. Remote Sens., 63, 1-14. doi.org/10.1109/TGRS.2024.1234567.